tions and extensions of these relations (*21*). Equation 1 offers some practical advantages, including provision for finite values of strain, strain rate, and strain acceleration at failure, as well as simplicity and ease of manipulation. Theory permits the deduction of time of failure, which may be applied in the interest of public safety.

REFERENCES AND NOTES

1. B. Voight and C. Faust, *Geotechnique* **32**, 43 (1982); B. Voight *et al.*, in *Proceedings of the International Symposium on Engineering Geology Related to Study, Preservation, and Protection of Ancient Works, Monuments, and Historical Sites* (International Association of Engineering Geology, Athens, in press), vol. 1. Although loading conditions were not constant at Vaiont (the reservoir adjacent to the failing slope had been raised, then twice lowered and raised again, and heavy rainfall had occurred), such load variations were less extreme in the weeks preceding ultimate collapse. In any case, failure could have been predicted over a week in advance by use of the analytical (say, Eq. 8) or graphical techniques presented here, a lead time sufficient to permit evacuation of communities at risk.
2. Earthquake instability models indicate that accelerating fault slip occurs at depth before instability, and is large enough to cause measurable rate changes in lengthening trilateration lines and creepmeter surveys [W. D. Stuart, *J. Geophys. Res.* **91**, 13771 (1986)]. The precursory interval is a fraction (perhaps 1 to 6%) of the loading or recurrence time. Thus measurable geodetic or precursory seismic rate changes could occur a few years or less before large and great earthquakes ($M = 7$ to 8), and such data could be evaluated by Eq. 1.
3. T. Fukuzono, in *Proceedings of the Fourth International Conference and Field Workshop on Landslides* (National Research Center for Disaster Prevention, Tokyo, 1985), pp 145–150.
4. B. Voight, *Eos* **68**, 1551 (1987); *ibid.*, p. 1286.
5. R. G. Campanella and Y. P. Vaid, *Can. Geotech. J.* **11**, 1 (1974).
6. B. F. Dyson and D. McLean, *Met. Sci.* **2**, 37 (1977).
7. The value of the dimensionless ratio $\Omega/\dot{\Omega}_0 t_f$ at failure is λ_f^*. Where Ω = strain, λ_f^* takes on the physical significance of ductility [I. N. Goodall, R. D. H. Cockroft, E. J. Chubb, *Int. J. Mech. Sci.* **17**, 351 (1975)]. For Eq. 6, $\alpha > 2$, $t = t_f$, one recovers $\lambda = \lambda_f^*$ and thus may obtain λ and α from a measurement of strain at failure [F. A. Leckie and D. R. Hayhurst, *Proc. R. Soc. London* **340**, 323 (1974)]. Values for α may likewise be determined from observed strain-time or rate-time relations. The equality $\lambda = \lambda_f^*$ holds only for $\alpha > 2$ and only for the simplified case in which $\dot{\Omega}_f$ is neglected. For $\alpha < 2$, λ is negative and $\lambda \neq \lambda_f^*$, although Eq. 6 nevertheless provides the appropriate form of the dimensionless curve, owing to contributions by the negative exponent $1/\lambda$. For $\alpha < 2$, Eq. 6 implies theoretical $\dot{\Omega}_f \rightarrow \infty$ and $\lambda^* \rightarrow \infty$ as $t \rightarrow t_f$. Obviously physically impossible, this is the consequence of neglect of $\dot{\Omega}_f$ in the simplified equations and may be resolved by use of the general equations.
8. F. H. Norton, *Creep of Steel at High Temperature* (McGraw-Hill, New York, 1929).
9. F. K. G. Odqvist and J. Hult, *Ark. Fys.* **19**, 379 (1961); R. K. Penny and D. L. Marriott, *Design for Creep* (McGraw-Hill, New York, 1971); F. A. Leckie and D. R. Hayhurst, *Acta Metall.* **25**, 1059 (1977). Such a rule is only approximate because the sequence of stresses can be important: early overloads may initiate cracks that accelerate failure at later decreased loads, but not conversely. (This is an example of the differing dominance of various mechanisms at different stages, which would change the "constants" A and α.)
10. Y. N. Rabotnov, *Creep Problems in Structural Members* (North-Holland, Amsterdam, 1969); L. M. Kachanov, *Izv. Akad. Nauk SSSR Otd. Tekh. Nauk* **8**, 26 (1958). The Kachanov concept of damage is widely used in applied mechanics, fitting the need for constitutive equations that represent important aspects of material behavior while retaining sufficient simplicity for mathematical manipulation. A more complete description would include microcrack shape and spatial attributes and associated distribution functions. This has been demonstrated both by experiment and by computer modeling, although the resulting equations are complex and the necessary tests difficult and time-consuming.
11. F. A. Leckie, *Philos. Trans. R. Soc. London Ser. A* **228**, 27 (1978); in *Mechanics of Engineering Materials*, C. S. Desai and R. H. Gallagher, Eds. (Wiley, New York, 1984), pp. 403–414. It is usually assumed that $\omega = 0$ when the material is undamaged and $\omega = 1$ at failure, although no precise definition of the Kachanov damage parameter ω is implied. These equations can be manipulated to predict rupture life for the situation of a uniaxial specimen subjected to constant strain rate ($t_R^{\dot{\varepsilon}}$), leading in the case $\nu = m$ to the expression $t_R^{\dot{\varepsilon}}/t_R = \lambda$, where t_R is rupture time under constant stress for the same minimum strain rate.
12. A. E. Johnson, J. Henderson, B. Khan, *Complex Stress, Creep Relaxation, and Fracture of Metallic Alloys* (Her Majesty's Stationery Office, Edinburgh, 1962).
13. F. C. Monkman and N. J. Grant, *Proc. Am. Soc. Test. Mat.* **56**, 593 (1956).
14. I. S. Servi and N. J. Grant, *Trans. Am. Inst. Min. Met. Eng.* **191**, 909 (1951).
15. F. Dobeš and H. Milička, *Met. Sci.* **1**, 382 (1976).
16. M. Saito, *Proc. 7th Int. Conf. Soil Mech. Found. Eng.* **2**, 677 (1969); S. Yamaguchi, *Rep. Sogu Doboku Lab.* (Tokyo) (1978), p. 14; D. J. Varnes, in *Proceedings of the 7th Southeast Asian Geotechnical Conference*, I. McFeat-Smith and P. Lumb, Eds. (Hong Kong Institution of Engineers, Hong Kong, 1983), vol. 2, pp. 107–130.
17. R. Sandström and A. Kondyr, *Proc. 3rd Int. Conf. Mech. Behav. Mater.* **2**, 275 (1980).
18. M. Saito and H. Uezawa, *Proc. 5th Int. Conf. Soil Mech. Found. Eng.* **1**, 315 (1961).
19. J. M. M. Ting, *Proc. Am. Soc. Civil Eng.* **109** [*J. Geotech. Eng.* 7], 932 (1983); Y. K. Zaretsky, B. D. Chuminev, V. I. Solomatin, *Eng. Geol. (Amsterdam)* **13**, 299 (1979).
20. A. C. F. Cocks and M. F. Ashby, *Prog. Mater. Sci.* **1**, 1 (1981); L. S. Costin, *Mech. Mater.* **4**, 149 (1985); A. Dragon and Z. Mroz, *Int. J. Eng. Sci.* **17**, 121 (1979); G. Greenwood, *Proc. Int. Cong. Met.* **2**, 91 (1973); D. Krachinovitz and G. V. Fonseca, *J. Appl. Mech.* **48**, 809 (1981); M. Lorrain and K. E. Loland, in *Fracture Mechanics in Concrete*, F. H. Wittman, Ed. (North-Holland, Amsterdam, 1983), pp. 106–111; A. R. S. Ponter and D. R. Hayhurst, Eds., *Creep in Structures* (Springer-Verlag, Berlin, 1981).
21. As a further example, a reviewer noted that an equation for primary creep, based on rate process theory for constant stress and temperature, can be written in the form $\dot{\varepsilon} = Bt^{-b}$, where B and b are constants. This may be expressed as $\dot{\varepsilon}^{-\alpha}\varepsilon = Dt^{b(\alpha-1)-1}$, where D is a derived constant. This conforms to Eq. 1 if $b(\alpha - 1) - 1 = 0$, implying for α about 2, a value for b of about unity. J. K. Mitchell, R. G. Campanella, and A. Singh [*Proc. Am. Soc. Civil Eng.* **94** (SM1), 249 (1968)] reported $0.75 < b < 1$ for tests for soils, implying that Eq. 1 may have a theoretical basis in rate process theory for primary creep.

22. I thank two anonymous reviewers for perceptive and extremely helpful comments.

14 April 1988; accepted 4 October 1988

Observation of Individual DNA Molecules Undergoing Gel Electrophoresis

STEVEN B. SMITH, PAUL K. ALDRIDGE, JAMES B. CALLIS

Individual DNA molecules undergoing agarose gel electrophoresis were viewed with the aid of a fluorescence microscope. Molecular shape and orientation were studied in both steady and pulsed electric fields. It was observed that (i) DNA macromolecules advanced lengthwise through the gel in an extended configuration, (ii) the molecules alternately contracted and lengthened as they moved, (iii) the molecules often became hooked around obstacles in a U-shape for extended periods, and (iv) the molecules displayed elasticity as they extended from both ends at once. A computer model has been developed that simulates the migration of the molecules in a rotating-field gel electrophoresis experiment.

THE ADVENT OF PULSED-FIELD GEL electrophoresis (PFGE) has allowed the separation of very large DNA fragments with relative ease (*1–3*), but the underlying molecular dynamics responsible for size separation have remained obscure. The prevalent model for describing DNA macromolecular motion, known as biased reptation (*4*), asserts that a very long DNA strand must snake its way through gel pores with one end leading and with the rest of the molecule following the same path. The path chosen by the head is assumed to be a semirandom walk, biased by the electric field force. The molecule is represented as a set of charged beads connected by freely orienting links. The gel pores are represented as a segmented tube surrounding the chain.

Deutsch (*5*) has recently published a series of computer simulations based on a new model also using a chain of beads but representing the gel as a lattice of point obstructions. Computer simulations based on these two models give different pictures of molecular motion. Unfortunately, direct experimental evidence concerning molecular orientation during electrophoresis, from fluo-

S. B. Smith, Department of Genetics SK-50, University of Washington, Seattle, WA 98195.
P. K. Aldridge and J. B. Callis, Center for Process Analytical Chemistry, Department of Chemistry BG-10, University of Washington, Seattle, WA 98195.

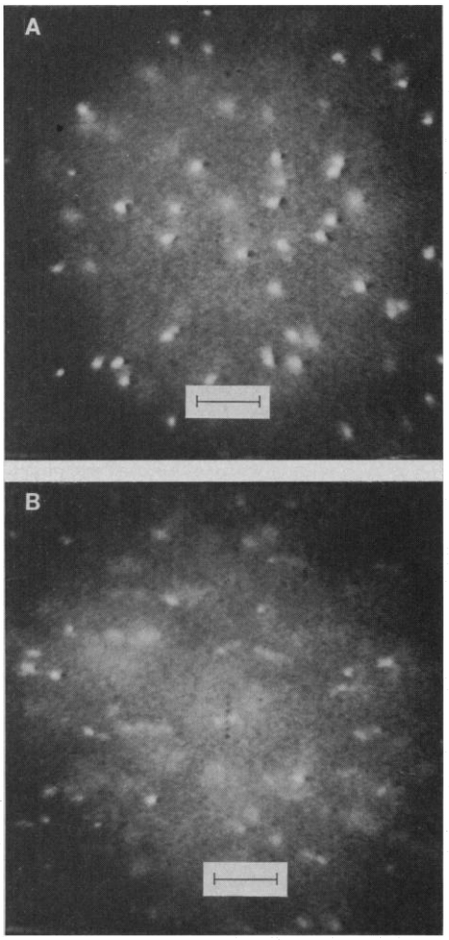

Fig. 1. Images of λ-phage DNA in agarose with (**A**) no electric field and (**B**) with 6 V/cm. A 1.5% agarose (SeaKem ME) suspension in 0.5× tris–boric acid–EDTA buffer (TBE) with 0.5 μg of ethidium bromide per milliliter was melted and brought to 60°C. Then 0.1 μg of λ-phage DNA (BRL) was added to 1 ml of agarose and 15 μl of the mixture was placed on a microscope slide preheated at 60°C. A 22-mm #1 cover glass was placed over the sample. After 5 min of cooling, it was coated on two opposite edges with fingernail polish. The microscope consisted of a Nikon MicroPhot FX with an epifluorescence attachment, a PlanApo 60× NA (numerical operative) 1.4 oil immersion objective, and a 2× magnifier. The depth of focus was 2 μm. The sample was excited in green light and viewed in red. A Varo Noctron 4 image intensifier, an Ikegami 310 vidicon television camera, and a Mitsubishi 359U VCR recorded the image. Infrared light from the excitation source was blocked by using a 3-mm Schott BG38 glass filter. The recorded video images were processed in a Quantex QX-7 image processing system coupled to an IBM PC/AT and photographed from the monitor screen. Each photograph is the average of four frames of NTSC video. Scale bar is 10 μm.

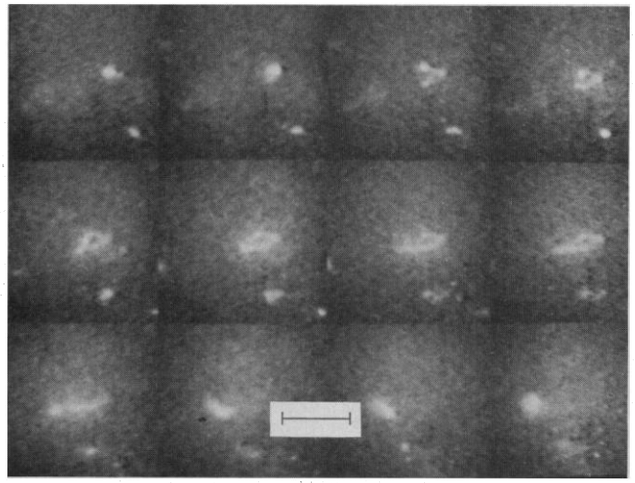

Fig. 2. Time sequence of a molecule of λ-phage DNA traveling toward the left in 1.5% agarose with a field of 8 V/cm. The frames are taken 0.4 s apart. The contour length of unstained λ-phage DNA is 15 μm, but the intercalating dye lengthens it. Scale bar is 10 μm.

rescence polarization and birefringence (*6*), has been difficult to interpret.

Our experimental approach is based on the pioneering work of Yanagida (*7*), who first observed individual DNA molecules that were stained with dye in a fluorescence microscope. Although the molecular details of DNA were not visualized, the general shape of the chain was resolved along its length to the Rayleigh limit imposed by the microscope objective used. The stained DNA molecules can be observed with the dark-adapted eye and even photographed, but the moving images are better captured with an image intensifier, television camera, and video tape recorder.

For microscopic observation of electrophoresis, thin layers of agarose, 10 to 20 μm thick, were cast under a cover slip onto a microscope slide. DNA stained with ethidium bromide had been premixed into the molten agarose.

In the absence of an electric field, the DNA could be seen tumbling and wiggling by Brownian motion in a thin liquid layer that formed just under the coverslip. DNA molecules embedded in the agarose appeared to be relatively motionless, however, with globular shapes ~2 μm across (Fig. 1A). The theoretical random coil diameter for λ-phage DNA is ~1 μm. The extra apparent diameter may be caused by blooming in the vidicon camera, which causes very bright objects to appear enlarged.

Fine platinum wires that formed the electrophoresis electrodes were placed adjacent to the cover slip and drops of buffer completed the electrical connection to the gel. In an electric field, λ-phage DNA molecules in the liquid layer tumbled and streamed rapidly toward the positive electrode. Molecules in the gel underwent a slower constrained motion, winding through invisible pores in the gel, elongating in the direction of the electric field, and then contracting as the tails caught up with the heads. In Fig. 1B the molecules are shown in various degrees of extension as they migrated in an electric field. With increasing field strength, the molecules became, on average, more extended and better aligned with the field.

The molecules often encountered obstacles such that both ends moved down field forming a U-shape. The time sequence in Fig. 2 shows a single molecule moving toward the left in a field and forming a U. After extending nearly to its contour length, the DNA molecule slipped free of the obstruction and moved into the path of the longer arm. This series of images shows a remarkable correspondence to those in figure 2 of Deutsch's report (*5*). When the electric field was suddenly removed, the extended arms of a U retracted toward the middle. This elasticity was probably caused by thermal motion randomizing the directions of persistence length segments inside the molecule (*8*). Evidently there was ample room inside the pores for the molecule to contract.

We next experimented with very long DNA chains such as yeast chromosomal DNA. To avoid shearing the DNA molecules, solid agarose microbeads containing treated yeast cells (*9*) were mixed with molten agarose and then cast into a thin gel. An electric field was applied, and whole chromosomal DNA molecules streamed from the beads into the bulk of the gel. These molecules, with contour lengths of several hundred micrometers (Fig. 3A), were more exactly aligned by an electric field than was λ-phage DNA. The same molecules, after relaxing 5 min without an electric field, had contracted to fill the pores in the agarose, making the gel voids and larger pores visible (Fig. 3B).

Size separation in orthogonal field agarose gel electrophoresis (OFAGE) is thought to depend on the way molecules realign when the electric field changes direction. In Fig. 4 yeast DNA is shown that had been undergoing electrophoresis toward the lower left when the field was suddenly rotated through an angle of 120°. In this case the molecules reversed their directions and the heads (which had been the tails) proceeded

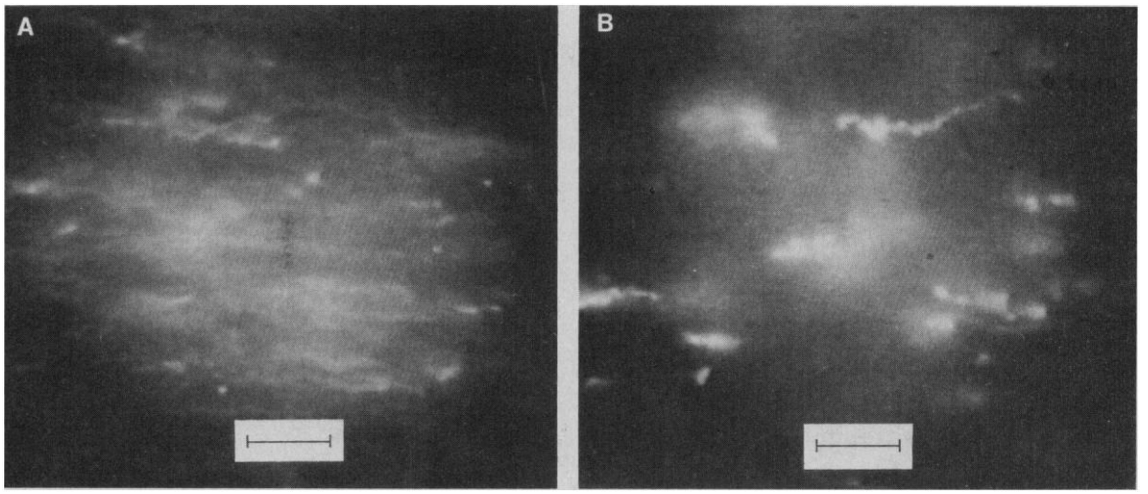

Fig. 3. Alignment of yeast DNA at (**A**) high field (7 V/cm) and (**B**) after relaxing in zero field for 5 min. Agarose microbeads containing *Saccharomyces cerevisiae* cells were treated to remove the cell walls and proteins (*9*). Ten microliters of bead suspension was added to 1 ml of molten (60°C) 1.5% SeaKem ME agarose in 0.5× TBE and 0.5 μg of ethidium bromide per milliliter. Fifteen microliters of the mixture was applied to a heated microscope slide and the cover glass was installed. Microbeads (not shown), each containing hundreds of cells, remained intact under the cover slip. Scale bar is 10 μm.

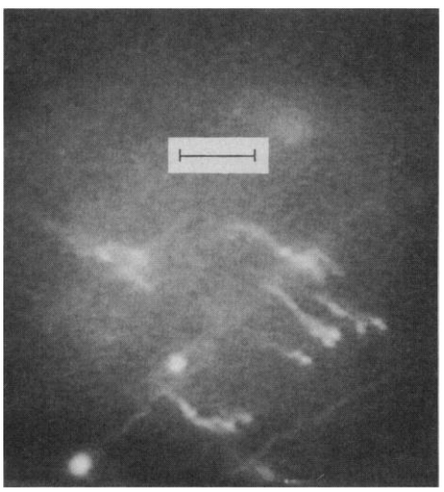

Fig. 4. Yeast DNA changing direction during OFAGE. A contour-clamped homogeneous electric field (CHEF) system (*10*) was constructed on a microscope slide. A computer with a digital-to-analog converter and multiplexer controlled the potential on 16 electrodes adjacent to the edges of the square cover slip. The direction and magnitude of the electric field were controlled with a joystick or cycled automatically. The electric field of 4 V/cm had changed direction by 120° 5 s before this picture was recorded. Scale bar is 10 μm.

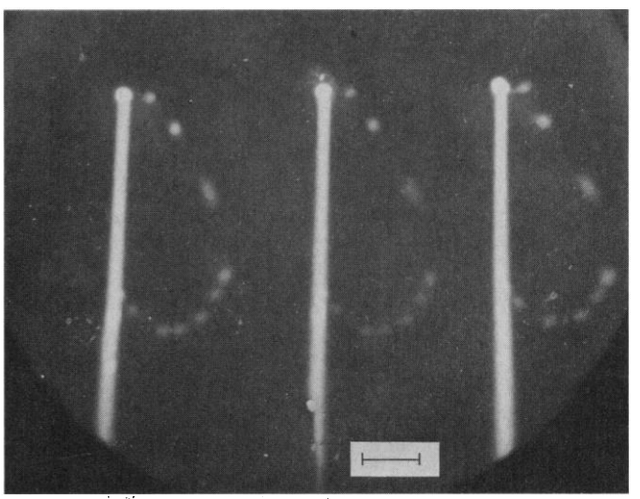

Fig. 5. Yeast chromosomal DNA separated by continuous rotation gel electrophoresis. DNA prepared in agarose beads was inserted in three round (2-mm) wells near the bottom of the photograph and run 24 hours in 1% SeaKem ME agarose 0.5× TBE buffer at 6°C. The electric field rotated clockwise (relative to the gel) at a constant rate of one revolution every 200 s. The field strength was 7 V/cm for the upper half of the revolution and 3 V/cm for the lower half. The bright vertical streaks are small fragments of chromosomes that escaped continually from the beads. The largest chromosomes, left of the wells (at bottom), are ~1200 kb in length and the smallest chromosomes that are still distinct from the streak (at top) are ~460 kb. Three smaller chromosomes are hidden in the streak (at top). Scale bar is 1 cm.

toward the lower right. Southern (*3*) predicted this sort of motion and showed how continually tacking the field would resolve molecular species by length. Our observations show that Southern's model was nearly correct, except where a constant-length chain was assumed. Usually both ends of the elastic molecule started off in the new field direction. In Fig. 4, the left ends of the molecules (which are not shown) may also be extending toward the lower right to form extended U shapes. Since such U's are slanted right in Fig. 4, the molecules slip off into the right arm when the contour length is nearly reached.

The leading end is usually the brightest part of a molecule in these experiments, suggesting that the DNA is bunched there. Apparently the body of a molecule can siphon through a path faster than the head can find new pores. For very long molecules, the head often has a forked appearance (Fig. 4), which is consistent with condensed DNA looping back on itself and moving through pores doubled over. Eventually the true end or one of the loops will "win" and pull all of the other loops backward through their pores until they straighten out and disappear.

Our observations agree with the computer simulation of Deutsch in several ways: the molecules fluctuate between compact and extended states during electrophoresis, extend farthest in the U configuration, go through pores doubled up in loops, appear to be elastic, and become compact at the leading end.

Our next endeavor was to see whether an empirical model that appeared correct on the microscopic scale would also give correct macroscopic DNA mobilities. One of us (S.B.S.) has simulated DNA motion using a reptation tube model with an elastic chain. The beads in this chain were spaced at 10-kbp intervals (66 persistence lengths). The forces on each bead included a random thermal force, an electric field force, and a springlike force between adjacent beads, thus simulating molecular elasticity. The velocity of a bead through the tube equaled the force component along the tube divided by a viscosity coefficient. The relative force strengths were chosen arbitrarily to make the simulated motion approach the molecular motion seen in the microscope (*11*).

A convenient test of these simulations has been a form of electrophoresis in which a

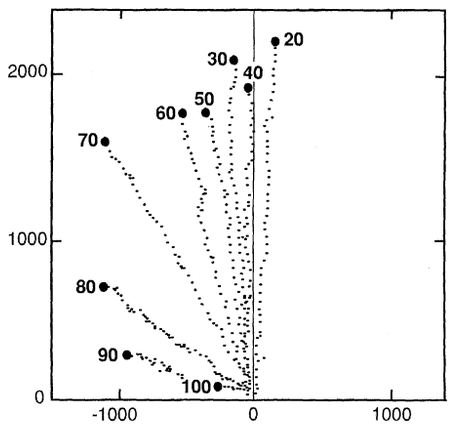

Fig. 6. Computer simulation of continuous-rotation gel electrophoresis. Nine simulated molecules ranging in size from 20 to 100 beads were started at the origin. Their paths were traced (dotted lines) for 50 revolutions of the electric field. The electric field rotated constantly with a period of 200 while the strength of the field was switched each half revolution between a value of 7 and 3. The axes are labeled with distance in units of maximal bead spacings, which, when compared with actual DNA contour length, correspond to 3 μm. This simulation ran 10 hours on an IBM PC/AT computer (*11*).

circular gel rotates continuously in a fixed-direction electric field. The mechanical setup is similar to Southern's (*3*), but instead of tacking between two fixed angles, the gel rotates at a constant rate and the electric field is switched between a high and low value every half revolution. The pattern of DNA migration, starting from three point sources, is shown in Fig. 5. The average direction of the electric field over time is straight up; it is in this direction that small DNA fragments travel (long streaks). The unexpected asymmetry of the pattern is caused by differences in the realignment rates of the molecules recently exposed to strong or weak fields. This characteristic pattern has been duplicated in tube-model simulations (Fig. 6). The simulation gives the correct lobe shape, that is, the correct angles and distances for the same relative size molecules. The model behaves correctly for different gel rotation rates, including the production of minor lobes at greater rates. Attempts are now being made to reproduce the resolving properties of field-inversion gel electrophoresis (*2*).

With readily available equipment, we have made observations of individual strands of DNA undergoing electrophoresis in pulsed and constant electric fields. Our images bear remarkable resemblance to simulations based on independently developed models. Investigations directed toward improving separations of large DNA strands are expected to advance rapidly with these new experimental techniques. A videocassette recording showing molecular motion is available for education and research (*12*).

REFERENCES AND NOTES

1. D. C. Schwartz and C. R. Cantor, *Cell* **37**, 67 (1984).
2. G. F. Carle *et al.*, *Science* **232**, 65 (1986).
3. E. M. Southern, R. Anand, W. R. A. Brown, D. S. Fletcher, *Nucleic Acids Res.* **15**, 5925 (1987).
4. L. S. Lerman and H. L. Frisch, *Biopolymers* **21**, 995 (1982); O. J. Lumpkin and B. H. Zimm, *ibid.*, p. 2315; O. J. Lumpkin, P. Dejardin, B. H. Zimm, *ibid.* **24**, 1575 (1985); G. W. Slater and J. Noolandi, *ibid.*, p. 2181.
5. J. M. Deutsch, *Science* **240**, 922 (1988).
6. H. Hervet and C. P. Bean, *Biopolymers* **26**, 727 (1987); M. Jonsson, B. Akerman, B. Norden, *ibid.* **27**, 381 (1988).
7. M. Yanagida, Y. Hiraoka, I. Katsura, *Cold Spring Harbor Symp. Quant. Biol.* **47**, 177 (1982).
8. F. Bueche, *Physical Properties Of Polymers* (Interscicence, New York, 1962).
9. G. F. Carle and M. V. Olson, *Methods Enzymol.* **155**, 468 (1987).
10. G. Chu, D. Vollrath, R. W. Davis, *Science* **234**, 1582 (1986).
11. A Pascal source code printout is available on request.
12. VHS cassettes entitled "Individual DNA Molecules Undergoing Gel Electrophoresis" can be obtained from Instructional Media Services, SB-54, University of Washington, Seattle, WA 98195.

13. We thank B. Shapiro for lending us his image intensifier.

16 August 1988; accepted 18 October 1988

Correct Folding of Circularly Permuted Variants of a βα Barrel Enzyme in Vivo

KAROLIN LUGER, ULRICH HOMMEL, MARZELL HEROLD, JAN HOFSTEENGE, KASPER KIRSCHNER*

An important question in protein folding is whether the natural amino and carboxyl termini and the given order of secondary structure segments are critical to the stability and to the folding pathway of proteins. Here it is shown that two circularly permuted versions of the gene of a single-domain βα barrel enzyme can be expressed in *Escherichia coli*. The variants are enzymically active and are practically indistinguishable from the original enzyme by several structural and spectroscopic criteria, despite the creation of new termini and the cleavage of a surface loop. This novel genetic approach should be useful for protein folding studies both in vitro and in vivo.

THE THREE-DIMENSIONAL STRUCTURE of a native protein is determined by its amino acid sequence (*1*), but it is unknown why and how a given polypeptide chain folds (*2*). From the comparison of the structures of homologous single-domain proteins and from reassembly studies with protein fragments, it appears that secondary structure segments that make up the internal core of a protein—and not the surface loops—are responsible for its stability (*3, 4*). One view of the folding mechanism envisages multiple routes involving partially folded intermediates with local nativelike structure (*5*). These folded regions are thought to consist mainly of secondary structure segments that are adjacent in the sequence.

Kinetic studies of the folding of mutant or homologous sequences have contributed importantly toward understanding protein folding (*2*). A more radical perturbation of the sequence is to rearrange the order of secondary structure segments by circular permutation; that is, by linking the natural amino and carboxyl termini through a new peptide bond and by cleaving one of the existing surface loops to create new termini. The sequence of bovine pancreatic trypsin inhibitor was the first to be permuted circularly by chemical condensation and limited proteolysis (*6*). However, this approach is not readily applicable to other proteins. It also provides no information on protein folding in vivo. We propose that circular permutation of the corresponding structural gene is a specific and versatile approach for varying the connectivity of secondary structure segments in a systematic manner and for producing the corresponding protein variants in bacteria. To demonstrate the feasibility of this novel approach, we constructed two different circular permutations of the structural gene. These genes were expressed in *Escherichia coli*, and the corresponding proteins were purified to homogeneity. Several structural and functional properties of these circularly permuted proteins show that they fold to a compact structure that is similar to that of the wild-type enzyme.

The structure of phosphoribosyl anthranilate isomerase from *Escherichia coli* (ePRAI), which is part of a bifunctional enzyme, has

K. Luger, U. Hommel, M. Herold, K. Kirschner, Abteilung Biophysikalische Chemie, Biozentrum der Universität Basel, Klingelbergstrasse 70, CH-4056 Basel, Switzerland.
J. Hofsteenge, Friedrich Miescher Institut, P.O. Box 2543, CH-4002 Basel, Switzerland.

*To whom correspondence should be addressed.